Performance evaluation of a solar adsorption cooling system under Mediterranean climatic conditions for cold stores applications

A. Mostafa[1,2], M. Hassanaina[1,*], E. Elgendy[3]

[1] Mechanical Power Engineering Department, Faculty of Engineering at El-Mattaria, Helwan University, Cairo, Egypt.

[2] Energy and Renewable Energy Engineering Program, Faculty of Engineering and Technology, Egyptian Chinese University.

[3]Mechanical Engineering Department, College of Engineering and Technology-Cairo Campus, Arab Academy for Science, Technology and Maritime Transport (AASTMT), Egypt.

Abstract

Today, energy and environmental issues have become major global concerns. Refrigeration and air conditioning systems account for a large share of world energy consumption. Reducing this energy consumption will not only reduce the energy crisis, but also reduce global warming by reducing carbon dioxide emissions from electricity generation. Compared with traditional refrigeration systems, the use of solar-assisted vapor adsorption refrigeration systems can not only reduce energy consumption, but also reduce the impact of the system on the environment. In this paper, a simulation study of a solar-assisted adsorption cooling system for refrigeration applications is carried out under Al Arish (31°N, 33.8°E) climatic conditions representing Mediterranean climate conditions in Egypt. The reported results revealed that the highest cold storage load occurred in August, while the highest COP of 0.54 and solar fraction of 0.86 occurred in May and June, respectively. In fact, based on annual system performance, the system consumes 5 x 107 kJ of energy through the auxiliary heater and harvests 1.8 x 10^8 kJ of solar energy to remove 1x 10^8 kJ of cold storage cooling load.

Keywords: Adsorption system; transient simulation; cold store; hot weather; cold store load.

***Corresponding Author Hassanain.100@gmail.com**

Nomenclature

C	specific heat (kJ/kg.k)
G	global solar radiation (W/m2)
M	mass (kg)
P	power (W)
Q	heat energy (kJ/h)
R	respiration rate (kJ/kg)
T	temperature (˚C)
V	volume (m^3)
Z	daily number of air exchange
c	heat load from a worker (W)

Greek symbols

ρ	density (kg/m^3)

Subscripts

amb	ambient
avg	average
Chilled	chilled water energy
cooling	cooling tower water energy
heater	heater energy
hot	hot water energy
i	inner
inf	infiltration
p	product
resp	respiration
Solar	solar heat gain

Acronyms

ARS	adsorption refrigeration systems
COP	coefficient of performance
CPC	concentrated parabolic collector
PER	primary energy ratio
SF	solar fraction
TF	turnover factor
HWCP	Hot water circulation pump

1. Introduction

Demand for energy is increasing as industries flourish and people's lives improve. Because electrically powered mechanical compression refrigeration is commonly utilized, cooling consumes around 10% of worldwide electricity [1]. Furthermore, the refrigerant used in mechanical compression refrigeration systems might contribute to global warming and ozone depletion. Because of the rapidly rising need for cooling, green refrigeration technology is critical. Adsorption refrigeration is popular because it may be powered by low-grade heat and uses natural refrigerants. As a result, it is ideal for sun cooling or industrial waste heat recovery. Furthermore, adsorption refrigeration has the benefits of being easy to manage, inexpensive in running costs, and producing less vibration. As a result, many academics and scholars throughout the globe are becoming more interested in adsorption refrigeration.

The purpose of a cold storage is to keep a product at a certain temperature while preventing quality loss. As a result, cold store customers have a strong incentive to minimize their energy use by implementing alternative solutions that are more energy efficient and have a lower environmental effect [2]. Solar adsorption cooling systems have been proven to be quite effective in addressing these issues. They do not utilize environmentally harmful refrigerants and do not rely on fossil-fuel-based energy. These cooling systems may be powered by low-grade energy sources such as solar energy, which is more widespread and uniformly distributed than other energy sources in nature. Additionally, the high solar radiation conditions throughout the summer, which nearly coincide with the times of anticipated peak cooling demand, make adsorption cooling a viable technique for sustainable energy consumption. Additionally, this technology may contribute to climate change mitigation by advancing toward the United Nations Sustainable Development Goal of achieving net-zero carbon emissions by the second half of the twenty-first century [3,4].

Adsorption cycles using silica gel/water or zeolite/water as working pairs have been found to be more effective than others when used in conjunction with solar panels or flat plate collectors since they may be powered at fairly low, near ambient temperatures [5-7]. The two-chamber design is often used for adsorption/desorption processes to allow the adsorption system to work alternately, resulting in an uninterrupted cooling cycle [8]. Numerous theoretical and technical advances have been made on water adsorbents such as silica gel and zeolite in order to optimize their use in adsorption cooling systems. Miyazaki and Akisawa [9] investigated the operational parameters of a single-bed silica gel–water adsorption system and discovered that, although increasing the size of the adsorbent bed reduces the coefficient of performance (COP) owing to the shorter cycle time, it also increases the specific cooling power (SCP). Chakraborty et al. investigated the effect of particle size and grain layers on the adsorption performance of silica gel numerically [10]. It is discovered that by using lower grain sizes, both COP and SCP may be increased. Freni et al. [11] investigated a new composite of silica modified with calcium nitrate and a water sorbent (SWS-8L), obtaining a COP of 0.18–0.31 for a 10 minutes cycle duration. Wang et al. [12] created a lumped-parameter model for a multi-bed silica

adsorption chiller and shown that adopting a multi-bed design enables the adsorption system to more efficiently use heat sources as low as 65°C than its mature two-bed technology. Manila et al. [13] shown by numerical modelling that a two-bed configuration with a shallower cylinder and an optimal silica gel grain diameter of 0.8 mm is preferred for increased vapor uptake and reduced bed pressure drop.

The ideal match between abundant sunshine and summer's peak cooling load demand indicates the greatest possible use of solar energy. As a result, the integration of solar collectors with adsorption systems has been widely studied in the literature. To increase the economic and technical feasibility of dual-stage absorption chillers in the building sector, Chemisana et al. [14] investigated the integration of highly efficient evacuated tube collectors with adsorptive chillers to achieve driving temperatures of up to 150°C and discovered that this configuration can result in a significant reduction in collector area requirements. Habib et al. [15] evaluated the one-stage and two-stage operation schemes of a four-bed silica gel-water adsorption system driven by evacuated tube collectors in Durgapur, India, using numerical simulations and discovered that the operation mode must be changed to dual-stage when the heat source temperature is less than (60°C). Drosou et al. [16] examined the potential of parabolic trough collectors for use with solar adsorptive refrigeration systems to meet the cooling requirements of a typical office building in Greece, demonstrating that this type of collectors can achieve a higher COP while occupying less space than traditional flat plate collectors. Wang et al. [17] investigated the effect of mass transfer on the performance of an activated carbon-methanol adsorption chiller and found that when the input radiation energy was not less than 14.7 MJ during a refrigeration cycle, the average COP of the natural mass transfer adsorption refrigeration system improved by 35.9 %.

It should be emphasized that most of the literature concentrated on the air conditioning use of the solar adsorption cooling system, leaving the cold storage of goods and food item application unexplored. Because of the scarcity of data on this application, the design characteristics of these systems must be discovered and analyzed for the cold storage use. Furthermore, few studies modelled the thermal loads of cold storage and its products under changing weather conditions over the course of a year. As a result, the purpose of this work is to simulate a solar aided adsorption refrigeration system used in a cold store to preserve fruits and vegetables. The suggested technique is critical in hot humid climate agricultural regions where mature fruits and vegetables must be kept at a low temperature. As a result, a costal arid city was chosen to represent hot humid climatic conditions of a lot of agriculture regions in middle east and north Africa as well as tropical regions.

2. SYSTEM DESCRIPTION

A schematic diagram of the investigated system is shown in Figure 1. The system consists of multiple subsystems such as solar field, adsorption refrigerator, and cold storage.

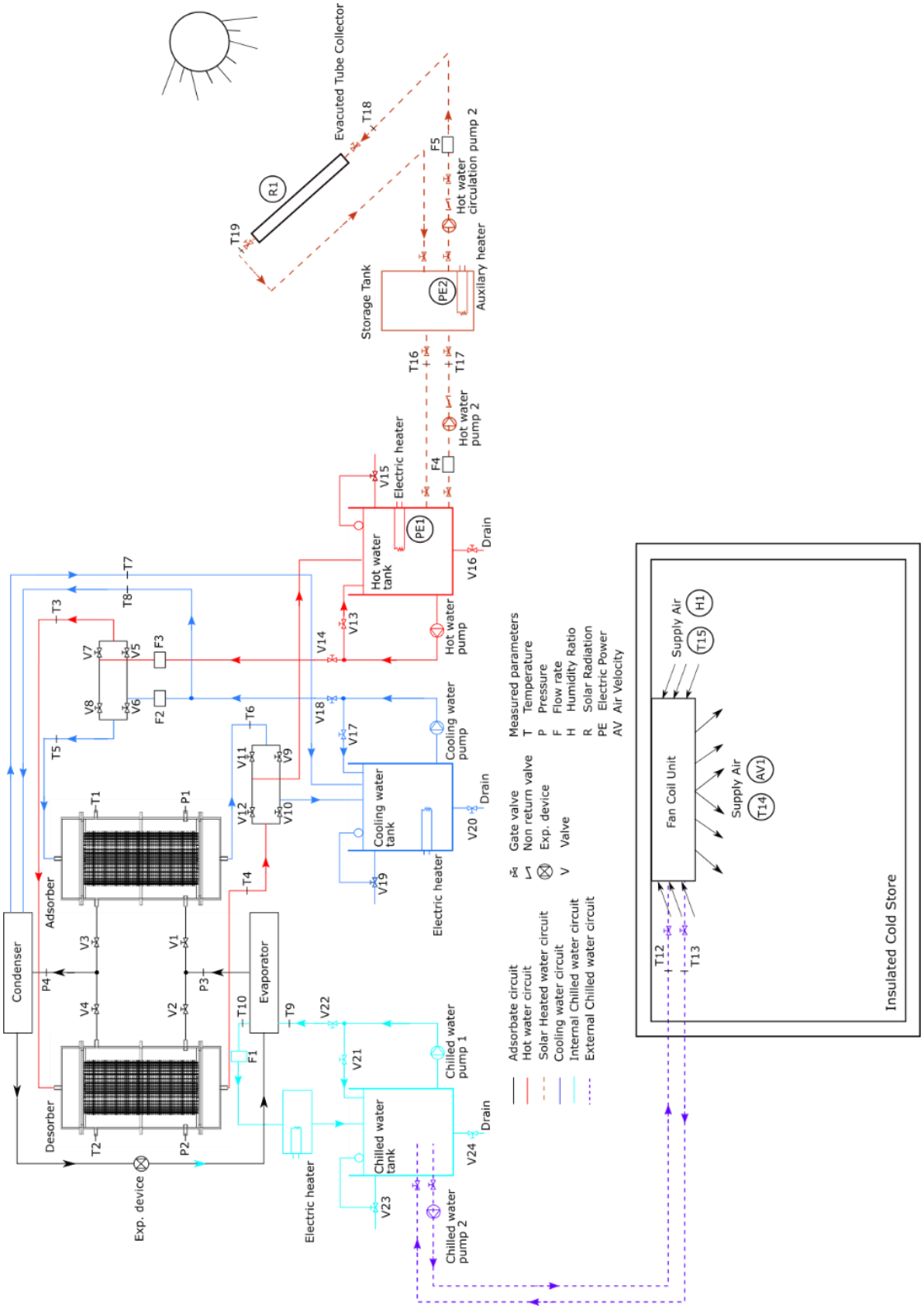

Figure (1) Schematic diagram for a solar assisted adsorption chiller utilized for a cold store.

2.1 Solar Field

An evacuated tube collector, a storage tank, water pumps, and an auxiliary heater with a thermostat are connected in a loop to form the solar field. The water circulation pump 2 (HWCP2) draws cold water from the storage tank and transports it to the flat plate collector, which transfers the heat to the hot water tank. However, the water circulation pump (HWCP1) is utilized to pull hot water from the hot water storage tank to the adsorption chiller's generator after passing it through the auxiliary heater to rise its temperature if necessary.

2.2 Adsorption Chiller

Two beds adsorption refrigeration system assisted by solar energy has been explored in the current study. The adsorption refrigeration cycle has four thermodynamic processes: (i) pre-cooling with depressurization (ii) adsorption followed by evaporation (iii) pre-heating and pressurization, and (iv) desorption followed by condensation processes. The adsorber/desorber heat exchanger beds are alternately connected to the hot water from the hot storage tank to heat the bed during desorption and pre-heating processes while the cooling tower is used to cool the beds during pre-cooling and adsorption processes. During both pre-cooling and pre-heating processes, the valve between the adsorber and the evaporator, as well as the valve between the desorber and the condenser, are closed. While during the adsorption and desorption processes, they are opened. The adsorption chiller in this research was intended to use silica gel and water as an adsorbent/adsorbate pair since this combination has been widely used for cooling processes powered by low-temperature heat sources (below 100˚C).

2.3 Cold Store

The simulated cold store volume is $60m^3$ with floor area of $42m^2$ and constructed from polyurethane sandwich panels. The panel is made from two sheets of metal 0.5mm thick each and a polyurethane insulation layer with a $40kg/m^3$ density and a thickness of 100mm. The cold store has a maximum capacity of 15000kg of vegetables or fruits. The percentage of worm products introduced to the cold store is estimated to be 10% of the total capacity and it called the turnover factor (TF). The cold store has two workers who spend two hours per day for handling the products inside the cold store. To illuminate the $42m^2$ of the cold store, four fluorescent lambs (200W) have been used during the working period of the products handling process. A fan coil unit with capacity 1500W has been used to circulate and cool the air inside the cold store.

3. SYSTEM SIMULATION AND PERFORMANCE CHARACTERISTICS

The simulation studio of TRNSYS-17 [18] is used to theoretically analyze the performance of the solar adsorption refrigeration system utilized for cold storage. The system composed of one air loop and four water loops with circulation pumps and fans. The water loops are solar collectors to the hot storage tank, hot storage tank to the adsorption chiller, cooling tower to the

adsorption chiller and adsorption chiller to the cold store fan coil unit while the air loop is between fan coil unit and cold store. Table 1 shows the key parameters and inputs for the TRNSYS simulation project.

3.1 Cold Store Load Estimation

To simulate the operation of the cold store, the cold store load must be calculated. Cold store load means the amount of heat removal from the cold store to maintain the required conditions. Therefore, the cold store load can be calculated as follows.

$$Q_{cold,store} = Q_{TR} + Q_{inf} + Q_{product} + Q_{resp} + Q_{person} + Q_{light} + Q_{fan} \quad (1)$$

The hourly transmission heat gain (Q_{TR}) has been calculated using TRNBUILD-17 (Type 56 module), which considers cold store dimensions, wall structure materials, cold store products heat capacitance and weather conditions. The other heat gain loads have been calculated hourly based on weather conditions and then coupled with the cold store model constructed in Type 56.

3.1.1 Infiltration heat gain (air change load)

The heat gained due to the entrance of the air with a higher temperature to the cold store through door openings is known as infiltration heat gain (Q_{inf}). This heat load can be calculated by using following equation [19].

Table (1) Simulation project key parameters.

TRNSYS type	Parameters and key inputs	Value	Unit
Type 909 – modified model for adsorption chiller	Design chilling capacity	8	kW
	Rated COP	0.6	-
	Fluid specific heat capacity	4.194	kJ/kg.k
	Manufacturer's performance data	SorTech ACS08	
	Rated hot water inlet temperature	55-95	˚C
	Chilled water outlet temperature	6-20˚C	˚C
	Cooling water temperature range	22-37˚C	˚C
Type 510 –cooling tower	Design air flowrate	5500	kg/h
	Fan maximum power	1.8	kW
Type 4a – hot storage tank	Volume	1.5	m^3
	Tank loss coefficient	0.8	$kJ/h.m^2K$
	Tank height	2	m
	Number of temperature nodes	10	-
Type 32 –fan coil unit	Number of rows	3	-
	Number of tubes	8	-
	Tube inner and outer diameters	13.2 and 12.3	mm

	Tube thermal conductivity	1443.6	kJ/h.m.K
	Fin thickness	0.11	mm
	Fin spacing	4.5	mm
	Fin thermal conductivity	738	kJ/h.m.K
	Centre to centre distance	2.5	cm
Type 112b– cold air fan	Rated flow rate	7000	kg/h
	Rated power	1.5	kW
	Motor efficiency	0.9	-
Type 3b – solar collector pump	Maximum flow	1000	kg/h
	Maximum power	0.430	kW
Type 3b -hot water pump	Maximum flow	1500	kg/h
	Maximum power	0.750	kW
Type 3b -cooling tower pump	Maximum flow	3300	kg/h
	Maximum power	1.5	kW
Type 3b -chilled water pump	Maximum flow	800	kg/h
	Maximum power	0.75	kW
Type 56 - cold store load	The cold store load simulation		

$$Q_{inf}= \rho_{air}\ Z\ V\ (h_{amb}-h_i)\ /24 \quad (2)$$

Where Q_{inf} is the heat gain from air changing due to the door openings (kJ/h), Z represents the number of daily air exchange is the cold store volume (m^3), h_i is the specific enthalpy of air at the storage temperature (kJ/kg) and h_{amb} is the specific enthalpy of air at the ambient temperature (kJ/kg).

3.1.2 Product heat gain

Most of the heat gain for the cold store is transferred when the warm harvested vegetables/fruits are initially brought into the cold store. The product heat gain can be calculated as follows.

$$Q_{product}=TF\ M_pC_p\ (T_{amb} - T_i)\ /24 \quad (3)$$

Where TF is the turnover factor, M_p is the product mass, C_p is the product specific heat, T_{amb} is the product initial temperature and T_i is the cold store temperature.

3.1.3 Respiration heat gain

Each vegetable/fruit has a heat of respiration which can be calculated by measuring how much CO_2 is generated per day then converting it to heat gain by the following equation.

$$Q_{resp}=M_p.\ R\ /24 \quad (4)$$

Where Q_{resp} is the respiration heat gain in (kJ/h) and R respiration rate for the product (kJ/kg).

3.1.4 Occupancy heat gain

The quantity of occupancy heat gain is determined by the number of people (n) and the length of time in hours they spend inside the cold store per day (t) as;

$$Q_{person}=n\ c_i\ t\ (24/1000) \quad (5)$$

Where c_i is the heat generated from one person (W).

3.1.5 Miscellaneous load

This load is mainly composed of the heat loads from electric lighting and cooler fan, which are computed in (kJ/h). The quantity of heat gained is determined by the number of pieces of utilized equipment (n), the number of hours per day that the equipment and lights are turned on (t), and the amount of heat generated by working equipment (W). These loads are determined using the following calculations.

$$Q_{light}= n\ P_{light}\ t\ (24/1000) \quad (6)$$

$$Q_{fan}= n\ P_{fan}\ t\ (24/1000) \quad (7)$$

3.2 System Performance Characteristics

The system performance is characterized by its coefficient of performance (COP), used solar fraction (SF) and primary energy ratio (PER). The actual adsorption chiller COP can be calculated as follows.

$$COP = Q_{cold,store}/ Q_{hot} \quad (8)$$

Where Q_{hot} is the heat supplied to the adsorption beds during pre-heating and desorption processes. The utilized solar fraction (SF) calculates the percentage of useful energy from the sun to the total thermal energy supplied to the adsorption beds (Q_{hot}) as **[26]**.

$$SF = \frac{Q_{hot} - Q_{heater}}{Q_{hot}} \quad (9)$$

Where Q_{heater} is the required auxiliary heater thermal energy (kJ).

4. RESULTS AND DISCUSSION

The transient simulation program has been applied on Al-Arish to represents Mediterranean weather conditions. Weather data for Al-Arish (latitude of 31.1321°N, longitude of 33.8033°E) is created using Meteonorm software version 7.0. The system transient simulation (with time step of 6 min) has been conducted during the peak month load to get the optimum design parameters. Furthermore, using the system design parameters listed in Table 2, the system performance has been evaluated monthly during the whole year. Finally, the accumulated yearly energy consumption has been compared.

Table (2) System design operating conditions

Parameter	Nominal value
Hot water inlet temperature (heater set point)	80˚C
Solar collector area	40 m^2
Collector inclination angle	30˚
Cold store set point temperature	15˚C
Collector water mass flow rate	1000 kg/h

4.1 Weather Data and Cold Store Load

The weather database accuracy is very important in the performance analysis of the solar cooling system. Figures 2 to 4 present the average daily relative humidity, dry bulb temperature and total solar radiation, respectively. It can be observed from the figures that, the daily average temperature and relative humidity of Al-Arish are relatively high. This mainly due to the costal nature of Al-Arish and its Aridity. It should be reported that highest daily average temperature is 33˚C occurred at day 202 (21stJuly) while the highest daily average relative humidity is 82 % at day 64 (5th March). The solar radiation follows the same trend as average daily average temperature during the year. The solar radiation reaches its maximum value of 840 W/m2 at day 183 (1st July) for Al-Arish.

Figure 6 indicates the monthly cold store cooling load at storage temperature of 15˚C. Clearly, the cold store cooling load increases in summer months due to the increase of ambient temperature. It can be observed from the figure that the highest storage cooling load is 1.45 x 10 ^{7}kJ in August.

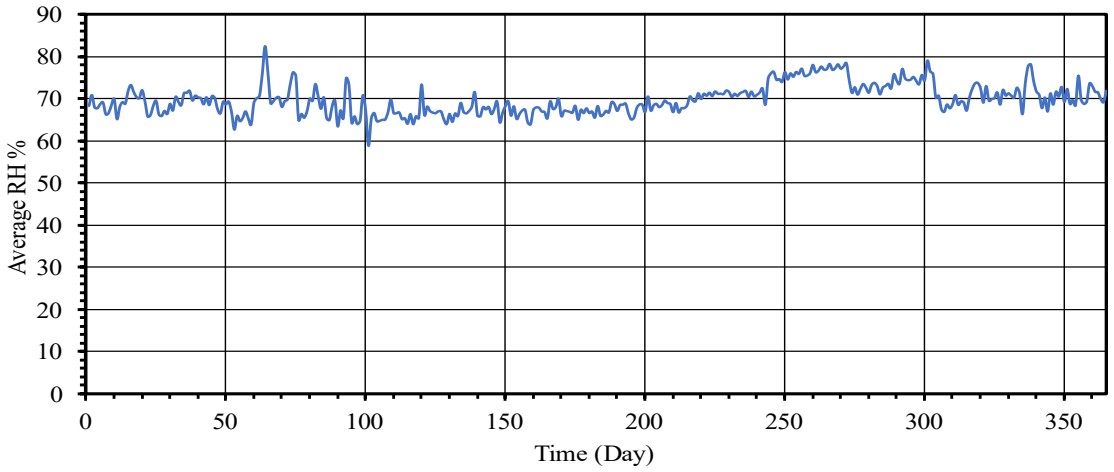

Figure (2) Variation of average daily relative humidity of Al Arish

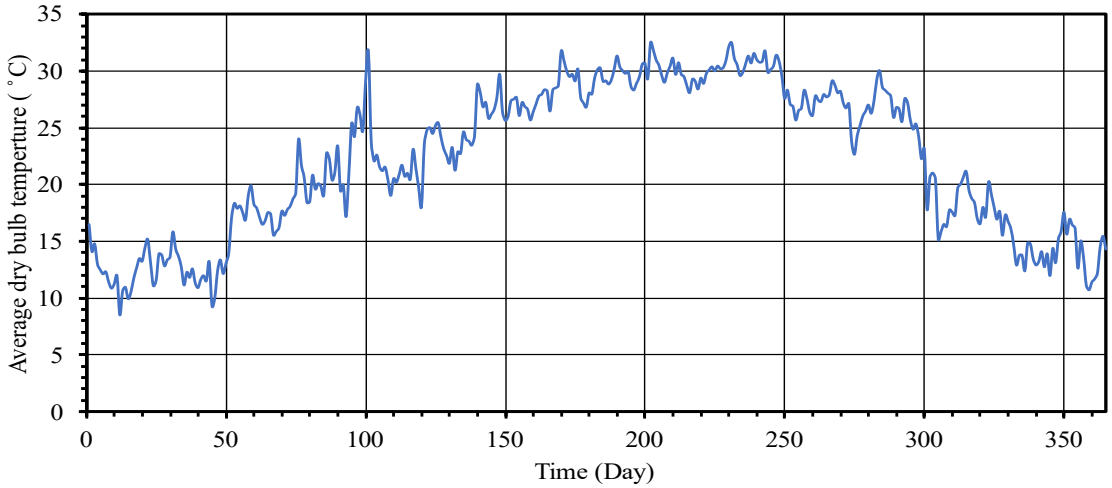

Figure (3) Al Arish average daily dry bulb temperature change

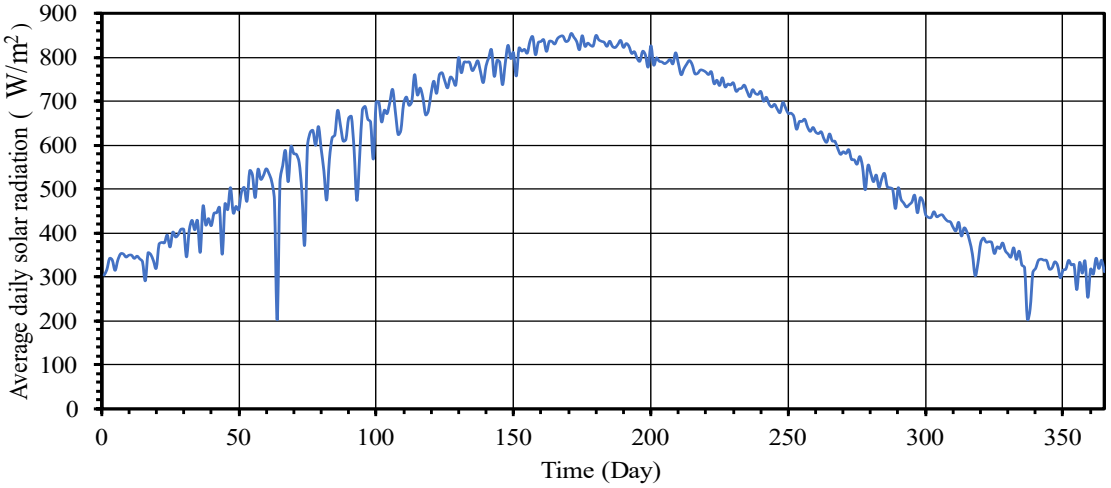

Figure (4) Daily average solar radiation of Al-Arish

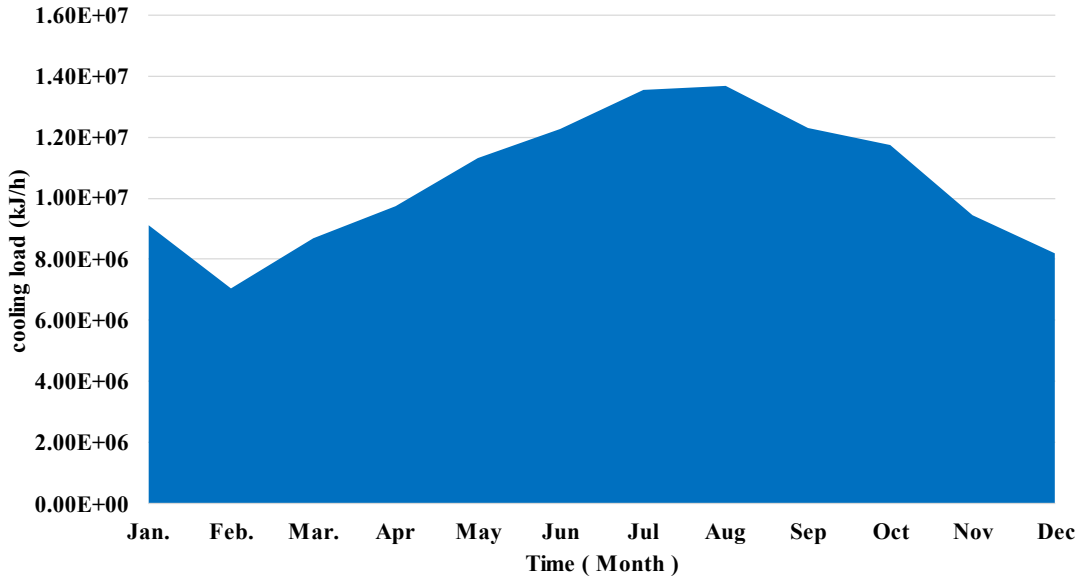

Figure (5) Monthly cooling loads of the cold store

4.2 System Transient Simulation

Figure 6 shows the hourly variation of system operating temperatures over a period of one week in August. Obviously during sun shining hours as collector outlet temperature is elevated, the hot storage tank outlet temperature is elevated gradually while chiller hot water inlet is fixed at heater setpoint temperature. This behavior continue till the hot storage outlet temperature reaches the heater setpoint and the heater is switched off and both temperatures are become equal and continue to elevate together till it reaches a peak value then it decreases again. Due to the utilizing of hot storage tank which store the useful solar energy from the collector, the hot storage outlet temperature decreases slowly, and the heater remains off after sunshine hours till it finally decreased below heater setpoint and the heater switched on again to prevent the chiller hot water inlet temperature to fall below heater setpoint.

Figure 7 presents a working cycle of the solar assisted cold store system explained by the behavior of the cold store temperature as well as the system rate of energies. The cycle starts by switching on the chiller when the cold store temperature reaches the upper differential limit of the controlling thermostat. When the chiller is turned on the chilled water energy rate will be at its peak and decreases gradually as cold store temperature decreases. At the same time, the chiller will consume the hot water energy supplied. If the hot storage outlet temperature is higher than the auxiliary heater set point, the heater will remain switched off and the chiller consumes heating energy from the energy stored in the hot storage otherwise the heater will be switched on to elevate the hot water temperature to the required value. The on cycle continues until the cold store temperature reaches the lower deferential limit and then the chiller and all its sub systems is switched off which means the rate of chilled water energy, rate of hot water energy, rate of cooling water energy and auxiliary heater energy will equal zero.

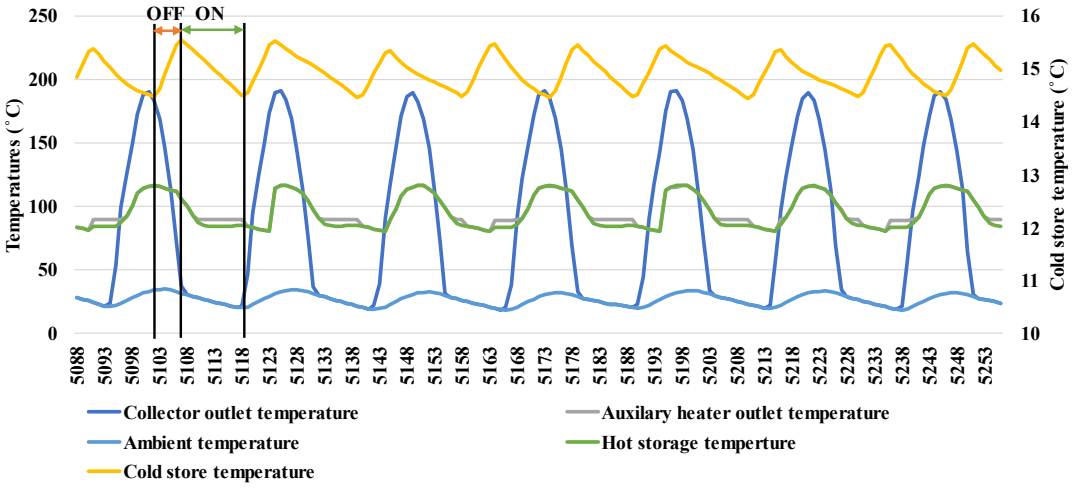

Figure (6) System operating temperatures hourly variation over a period of one week

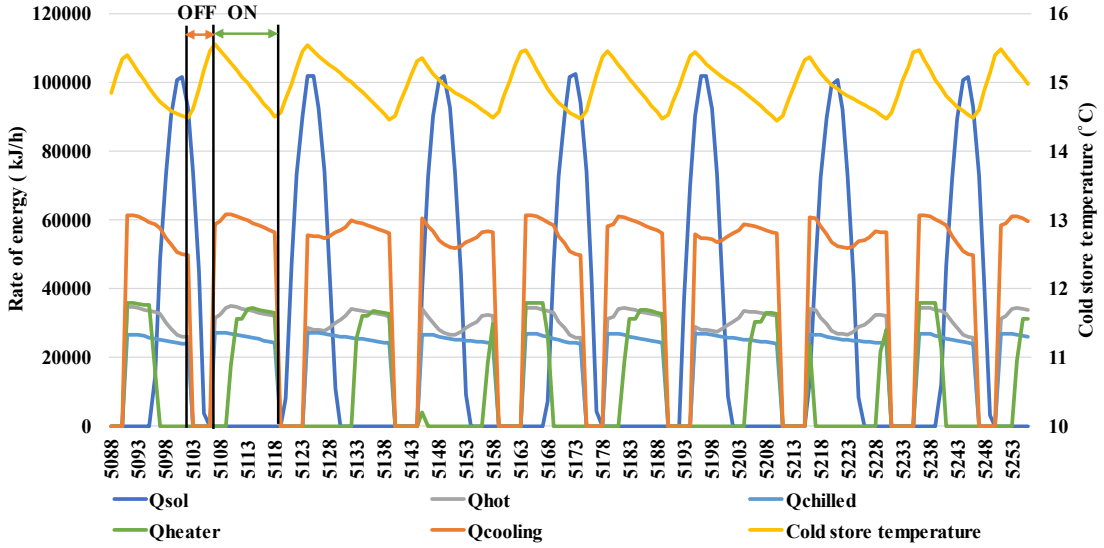

Figure (7) Variation of system energies hourly rate and cold store temperature over a period of one week

The chiller remains off while the cold store temperature starts to rise again due to the internal and external cooling loads of the store until it reaches the upper deferential limit of the controlling thermostat, and the cycle is then repeated.

4.3 Monthly System Performance

Variation of monthly system useful solar heat gain and chilled water load are shown in Figures 8 and 9. Clearly from the figure, both useful solar energy gain and chilled water load increase monthly to a maximum value in August and then decrease again. This is mainly due to the behavior of solar radiation and ambient temperature change as shown in Figures 3 and 4. It can be estimated from the figure that the peak useful solar gain in August is 2.5 times the minimum solar gain of December.

Change of monthly system COP is presented in Figure 10. Although the store cooling load is lower during winter, the system COP is higher during summer months. The primary reasons for this trend are increased solar radiation and consistent solar useful heat gain during the summer months, which raises the collector outlet temperature and corresponding hot water inlet temperature to the chiller, thereby increasing the desorption cycle in the chiller and thus the system COP. It can be seen from the figure that, the system COP varies between 0.45 and 0.55 during the year months and the highest system COP is 0.54 occurred in May.

Variation of monthly heater energy consumption is presented on Figure 11. It's clear from the figure that, the required heater energy in summer period is lower due to the high solar energy gained from the collector (see Figure 8). It can be noted from the figure that, the minimum monthly heater energy consumption is 3.5 x 10^6 kJ and occurs in June is 72% less than the highest consumption, which occurs in December.

Figure 12 presents the monthly solar fraction change. It's clear from the figure that, the SF has a similar trend to the solar radiation and is higher during summer months.

It should be reported that, the highest SF of 0.86 has been occurred in June. Figure 13 illustrates the monthly variation of chiller supplied hot energy. Due to the increase in solar radiation and the corresponding useful solar energy delivered to the system, the Q_{hot} is higher during summer period.

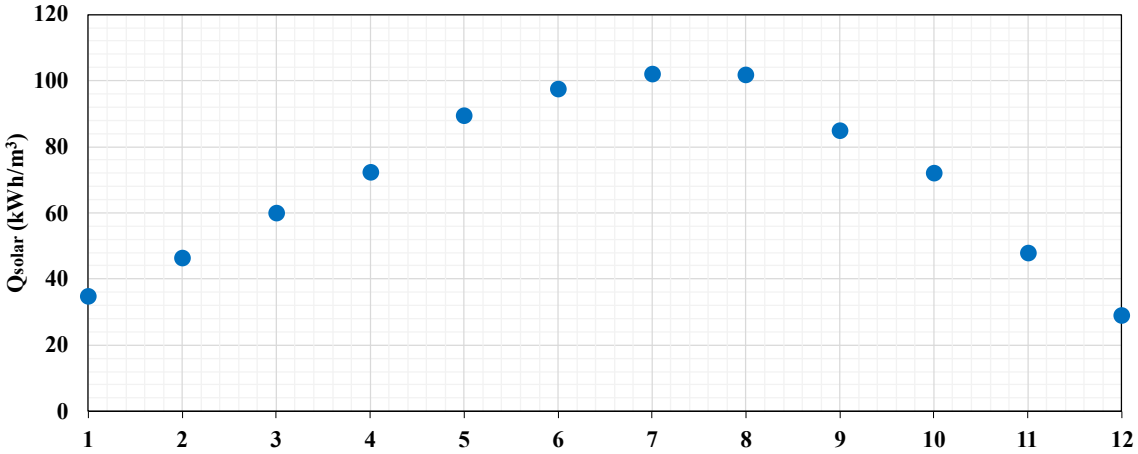

Figure (8) Monthly useful solar heat gain variation

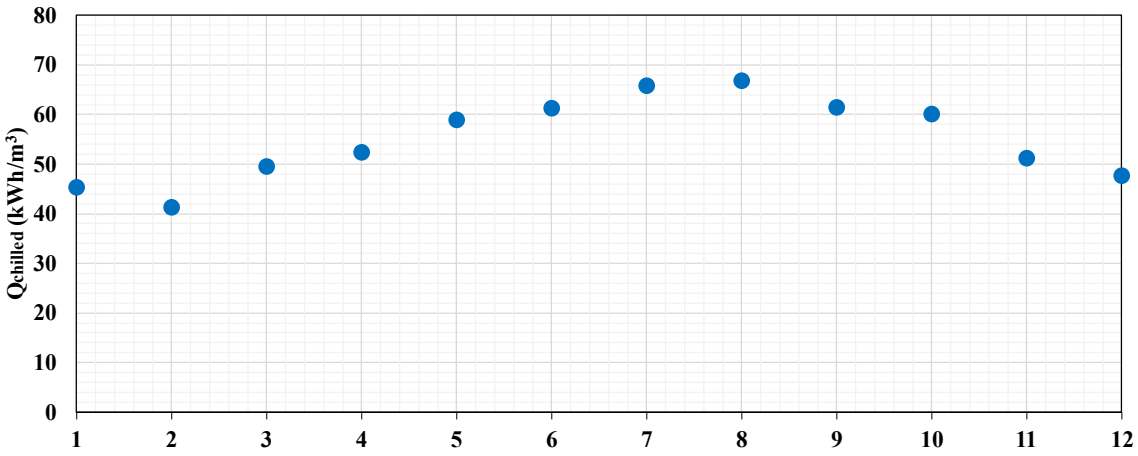

Figure (9) Monthly chilled water load variation.

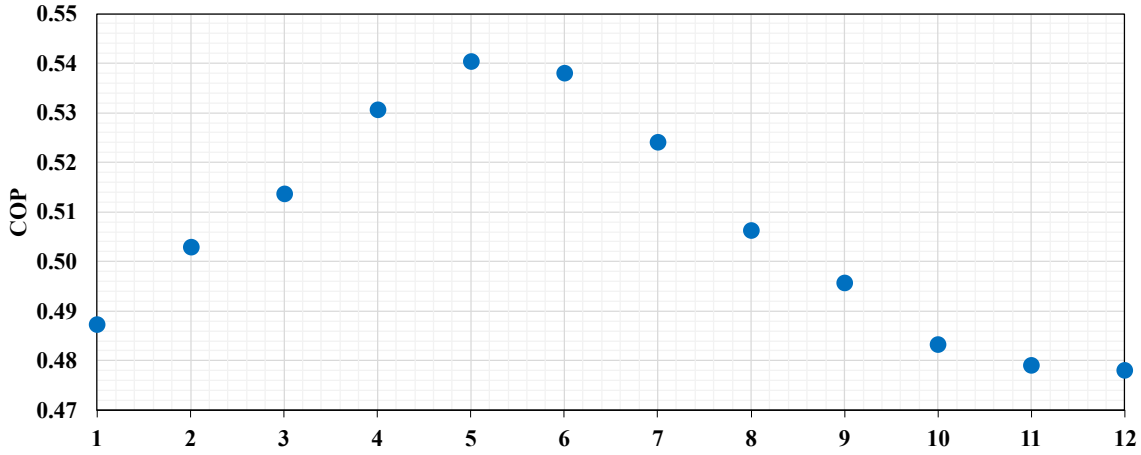

Figure (10) Variation of monthly system COP

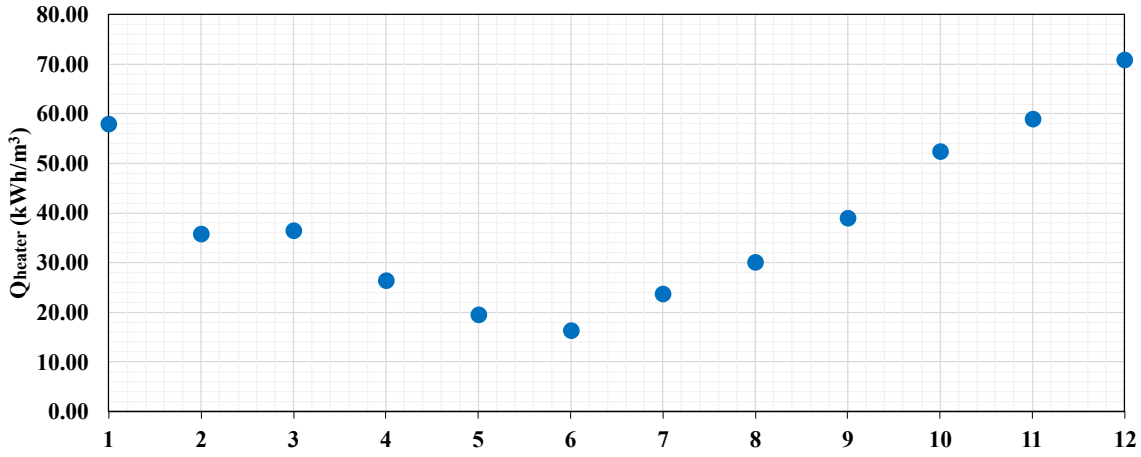

Figure (11) Change of monthly heater energy consumption

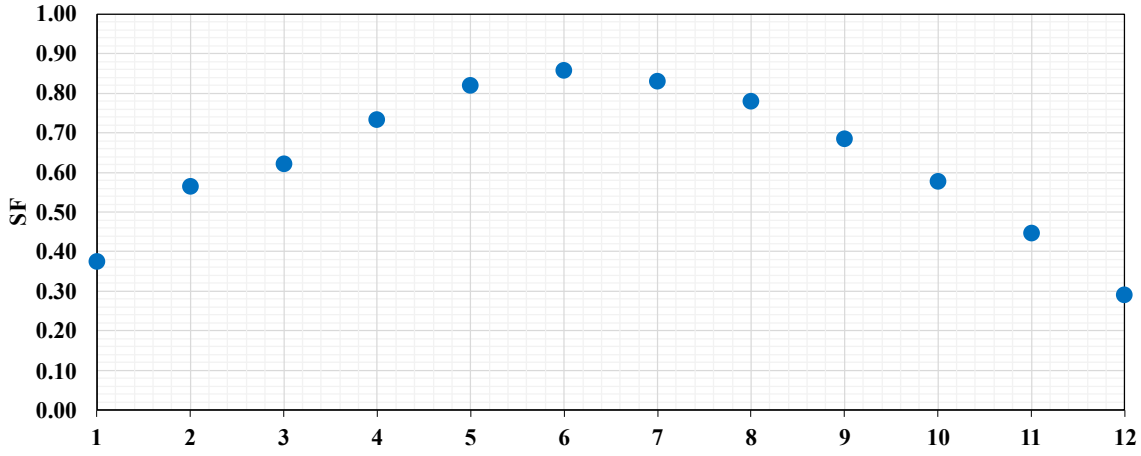

Figure (12) Monthly variation of solar fraction

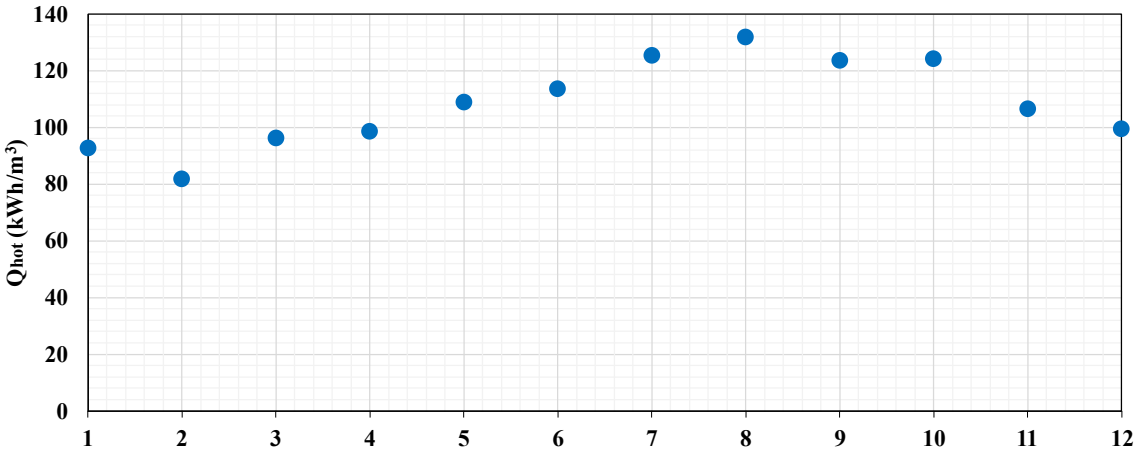

Figure (13) Variation of monthly chiller supplied hot energy

Conclusions

A transient simulation of a solar-assisted adsorption refrigeration system used in a cold store was carried out. Weather data for the city of Al-Arish (31.1321°N, 33.8033°E) was selected to represent hot and humid weather conditions. The simulated cold storage capacity is 60m^3. Based on the reported results, the following conclusions are drawn:

- The highest storage cooling load was 1.45 x 10 7kJ in August.
- The peak useful solar gain in August is 2.5 times the minimum solar gain in December.
- The highest system COP of 0.54 occurred in May, while the highest SF of 0.86 occurred in June.
- The heaters in June consumed the lowest energy at 3.5 x 106 kJ, which was 72% lower than the peak consumption in December.
- To maintain the cold store at set temperature of 15˚C, a 1x10^8 kJ of cold store load must be removed yearly by consuming a 5x10^7 kJ of energy via the auxiliary heater at an average system COP of 0.5 as well as harvesting a 1.8x108 kJ of energy yearly through solar collectors at an average system solar fraction of 0.65.

References

[1] International Energy Agency. The Future of Cooling. 2018. https://www.iea.org/reports/the-future-of-cooling
[2] Rouf, R.A.; Jahan, N.; Alam, K.C.A.;Sultan, A.A. ;Saha, B.B. ;Saha, S.C. Improved cooling capacity of a solar heat driven adsorption chiller, Case Stud. Therm. Eng. 2020,17 , 100568.
[3] Masson-Delmotte, V.; Zhai, P.; Pörtner, H.-O.; Roberts, D.; Skea, J.; Shukla, P.R.; Pirani, A.; Moufouma-Okia, W.; Péan, C.; Pidcock, R. Global Warming of 1.5 C.

2018, 1. https://apps.ipcc.ch/outreach/documents/451/1551801374.pdf (accessed on 14 March 2022).
[4] Hassanpouryouzband, A.; Joonaki, E.; Edlmann, K.; Haszeldine, R.S. Offshore Geological Storage of Hydrogen: Is This Our Best Option to Achieve Net-Zero? ACS Energy Lett. 2021, 6, 2181–2186.
[5] Askalany, A.A.; Salem, M.; Ismael, I.M.; Ali, A.H.H.; Morsy, M.G.; Saha, B.B. An overview on adsorption pairs for cooling. Renew. Sustain. Energy Rev. 2013, 19, 565–572.
[6] Sah, R.P.; Choudhury, B.; Das, R.K. A review on adsorption cooling systems with silica gel and carbon as adsorbents. Renew. Sustain. Energy Rev. 2015, 45, 123–134.
[7] Shmroukh, A.N.; Ali, A.H.H.; Ookawara, S. Adsorption working pairs for adsorption cooling chillers: A review based on adsorption capacity and environmental impact. Renew. Sustain. Energy Rev. 2015, 50, 445–456.
[8] Alahmer, A.; Ajib, S.; Wang, X. Comprehensive strategies for performance improvement of adsorption air conditioning systems: A review. Renew. Sustain. Energy Rev. 2019, 99, 138–158.
[9] Miyazaki, T.; Akisawa, A. The influence of heat exchanger parameters on the optimum cycle time of adsorption chillers. Appl. Therm. Eng. 2009, 29, 2708–2717.
[10] Chakraborty, A.; Saha, B.B.; Aristov, Y.I. Dynamic behaviors of adsorption chiller: Effects of the silica gel grain size and layers. Energy 2014, 78, 304–312.
[11] Freni, A.; Sapienza, A.; Glaznev, I.S.; Aristov, Y.I.; Restuccia, G. Experimental testing of a lab-scale adsorption chiller using a novel selective water sorbent “silica modified by calcium nitrate”. Int. J. Refrig. 2012, 35, 518–524.
[12] Wang, X.; He, Z.; Chua, H.T. Performance simulation of multi-bed silica gel-water adsorption chillers. Int. J. Refrig. 2015, 52, 32–41.
[13] Manila, M.R.; Mitra, S.; Dutta, P. Studies on dynamics of two-stage air cooled water/silica gel adsorption system. Appl. Therm. Eng. 2020, 178, 115552.
[14] Chemisana, D.; López-Villada, J.; Coronas, A.; Rosell, J.I.; Lodi, C. Building integration of concentrating systems for solar cooling applications. Appl. Therm. Eng. 2013, 50, 1472–1479.
[15] Habib, K.; Choudhury, B.; Chatterjee, P.K.; Saha, B.B. Study on a solar heat driven dual-mode adsorption chiller. Energy 2013, 63, 133–141.
[16] Drosou, V.; Kosmopoulos, P.; Papadopoulos, A. Solar cooling system using concentrating collectors for office buildings: A case study for Greece. Renew. Energy 2016, 97, 697–708.
[17] Wang, Y.; Li, M.; Ji, X.; Yu, Q.; Li, G.; Ma, X. Experimental study of the effect of enhanced mass transfer on the performance improvement of a solar-driven adsorption refrigeration system. Appl. Energy 2018, 224, 417–425.
[18]Klein, S.A. et al. TRNSYS 17: A Transient System Simulation Program, SolarEnergy Laboratory, University of Wisconsin, Madison, USA, 2016.
[19] ASHRAE, “ASHRAE Handbook Refrigeration”, Atlanta: American Society of Heating, Refrigeration, and Air Conditioning Engineers Inc, 2015.